Theor Chem Acc (1997) 96:114–121

Theoretical
Chemistry Accounts

A model VBCI calculation on the state correlation diagram for radical abstraction and addition reactions

A. Salikhov, H. Fischer

Physikalisch-Chemisches Institut, Universität Zürich, Winterthurerstrasse 190, CH-8057 Zürich, Switzerland

Received: 8 November 1996 / Accepted: 5 March 1997

Abstract. State correlation diagrams for radical reactions are calculated from potential energy surfaces for the model process $A-B+C \rightarrow A+B-C$ including the $H-H+H$ reaction of three one-electron atoms with ab initio valence bond configuration interaction in a minimal 1s basis. Effects of substituents are simulated by a variation of the nuclear charges. Qualitative predictions derived from the diagrams agree well with recent experimental and advanced theoretical data. In general, the reaction barrier and the geometry of addition and abstraction reactions depend strongly on the reaction enthalpy, but there are marked exceptions if charge transfer states of the reactants have particularly low energies.

Key words: Valence bond theory – State correlation diagram – Variable charges – Polar effect – Enthalpy effect

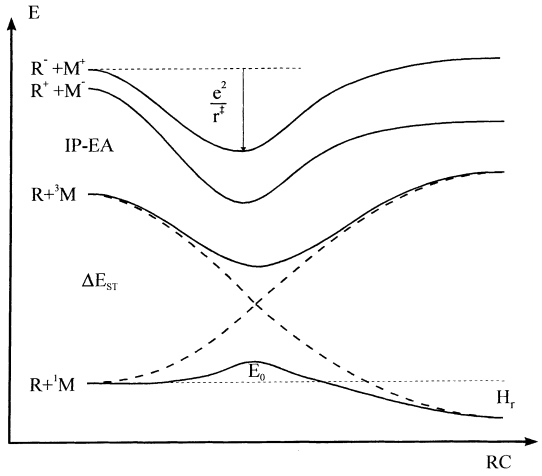

Fig. 1. Schematic state correlation diagram (SCD) for radical abstraction and addition reactions

1 Introduction

The course and the barriers of chemical reactions are often conveniently discussed in terms of the correlation of reactant and product states [1]. To construct a state correlation diagram (SCD) for radical abstraction and addition reactions, in particular,

$$R\cdot + X-Y \rightarrow R-X+Y\cdot$$
$$R\cdot + X=Y \rightarrow R-X-Y\cdot$$

one considers the doublet states of a model three-electron system formed by the initially unpaired radical electron and the electron pair of the attacked bond [2–5]. From spin pairing schemes [2–5] and simple valence bond arguments [3, 6] it is qualitatively concluded that the energies of the lowest reactant states should develop along the reaction coordinate as shown schematically in Fig. 1, where the attacked molecule is abbreviated as M. In the absence of configuration interaction the energy of the reactant ground state with the singlet bonding electron pair on M approaches the first excited state of the product, whereas an unpolar excited reactant state with a triplet electron pair on M approaches the product ground state (broken lines). The mixing of these states causes an avoided level crossing and explains the barrier E_0. Furthermore, polar charge transfer states of the reactants are stabilized on approach of the species by the Coulomb attraction. They mix with the unpolar states [3, 5, 6], and this lowers E_0. This SCD allows important predictions on the influence of parameters of the reacting systems on the reaction barriers. With increasing reaction exothermicity $(-H_r)$ and decreasing singlet-triplet energy gap (ΔE_{st}) of M the barrier E_0 should decrease and, simultaneously, the distance between the reactants in the transition state should increase. In addition, the polar charge transfer effects will be important if and only if the energies of the reactant charge transfer states IP(R)-EA(M) and IP(M)-EA(R) are low. This should become apparent by correlations of E_0 with the ionization potentials (IP) and electron affinities (EA) of the reacting species.

Recently, these predictions have been nicely verified for additions of several alkyl radicals to various mono-

Correspondence to: H. Fischer

and 1,1-disubstituted alkenes both by high-level theory [7] and experiment [8]. In most cases the variation of the reaction barriers with alkene substitution was found to be dominated by the changes of H_r, but for some radicals with very low IP or high EA the polar effects of low-lying charge transfer states play the deciding role [8, 9].

Here, we present a theoretical valence bond configuration interaction (VBCI) study which aims at a better understanding of the inner working of the SCD for the three-center three-electron model of radical reactions. We consider the reaction of three one-electron atoms $A{-}B + C \rightarrow A + B{-}C$ in a linear arrangement, and use a minimal 1s basis set of orbitals a, b, c at the atoms. In the full VBCI calculation all eight possible doublet states are taken into account. The integrals are evaluated exactly within the STO-6G frame. To vary the relevant energies $H_r, \Delta E_{st}$ and IP-EA, i.e. to approximate substituent effects in radical reactions, the nuclear charges of the atoms are varied.

For unit nuclear charges our system is, of course, the linear $H_2 + H \rightarrow H + H_2$ reaction which has been studied extensively since 1929, with increasing levels of accuracy [10]. The potential energy surface (PES) for the electronic ground state is known theoretically to the experimental precision [11] of about 1 kj/mol which can not be reached here. Therefore, we will only compare our minimal basis VBCI results with similar earlier calculations. More related to this work are the constructions of SCDs for the $H_2 + H$ reaction by Bonačič-Koutecký et al. [3], Shaik et al. [6] and by Klessinger and Höweler [12] and for $H_2 + H_2$ by Gerhartz et al. [13] from which this work differs in the choice of the diabatic reference functions, the evaluation of the integrals and the simulation of substituent effects.

2 Computational method

The atoms A, B and C carry nuclear charges Z_A, Z_B and Z_C, and possess one 1*s* orbital *a*, *b* and *c* each. The three electrons occupy these orbitals with occupation numbers 0, 1 and 2. The wavefunctions are constructed from the following linear combinations of Slater determinants corresponding to doublets with $M_s = +1/2$. They represent physically meaningful electronic configurations of the reactants at infinite separation:

$$\varphi_1 = N_1(\| a\bar{b}c \| + \| b\bar{a}c \|)$$
$$^1AB + C \quad \text{AB covalent ground state,} \tag{1a}$$

$$\varphi_2 = N_2(\| a\bar{b}c \| - \| b\bar{a}c \| + 2\| a\bar{c}b \|)$$
$$^3AB + C \quad \text{AB covalent triplet state,} \tag{1b}$$

$$\varphi_3 = N_3(\| a\bar{c}c \| + \| b\bar{c}c \|)$$
$$^sAB^+ + C^- \quad \text{AB polar symmetric,} \tag{1c}$$

$$\varphi_4 = N_4(\| a\bar{a}c \| - \| b\bar{b}c \|)$$
$$^aA^-B^+ + C \quad \text{AB zwitterionic asymmetric,} \tag{1d}$$

$$\varphi_5 = N_5(\| a\bar{a}b \| + \| a\bar{b}b \|)$$
$$^sAB^- + C^+ \quad \text{AB polar symmetric,} \tag{1e}$$

$$\varphi_6 = N_6(\| a\bar{a}c \| + \| b\bar{b}c \|)$$
$$^sA^-B^+ + C \quad \text{AB zwitterionic symmetric,} \tag{1f}$$

$$\varphi_7 = N_7(\| a\bar{c}c \| - \| b\bar{c}c \|)$$
$$^aAB^+ + C^- \quad \text{AB polar asymmetric,} \tag{1g}$$

$$\varphi_8 = N_8(\| a\bar{a}b \| - \| a\bar{b}b \|)$$
$$^aAB^- + C^+ \quad \text{AB polar asymmetric.} \tag{1h}$$

The covalent quartet configuration $\varphi_9 = N_9\ (\| a\bar{b}c \| - \| b\bar{a}c \| - \| a\bar{c}b \|)$ does not interact and is not considered further.

As is obvious from Fig. 1, a SCD represents the energies of Born-Oppenheimer states and of reference electronic states plotted together versus the reaction coordinate (RC). This implies that the calculation of a SCD requires the determination of the PESs, for both sets of states, the location of the RC on the PES of the lowest Born-Oppenheimer state, and the construction of the energy profiles of all states along RC. Our procedure involved the following steps: selection of a spatial grid for the PESs, calculation of the overlap integrals S_{ps}, the core integrals I_{ps} and the two-electron integrals (ps|qt) between the atomic orbitals $p, q, s, t \in \{a, b, c\}$ at each grid point, transformation of the integrals between the atomic orbitals into integrals between Slater determinants, addition of the nuclear Coulomb repulsion and collection of the data as matrix elements between the doublet basis functions φ_i, diagonalization of the VBCI matrix $H_{BO} - ES$, refinement of the PESs by interpolation, location of the reaction coordinate on the ground state PES and calculation of all energies and state vectors along the RC.

The linear reaction configuration was chosen, because it is known to give the minimum energy path for the $H_2 + H$ reaction [11]. For the calculation of SCDs the internuclear distances r_{AB} and r_{BC} were set to the values $r_{AB}, r_{BC} \in \{0.5, 0.6,$ step 0.05, 1.5, step 0.1, 2.0, step 0.2, 3.0, 3.5, 4.0, 5.0, 6.0 Å$\}$ giving 34^2 grid points. For more exact calculations of reactants, products and transition states a grid of smaller size but with finer spaces around the relevant geometries with $r_{AB}, r_{BC} \in \{0.675,$ step 0.025, 1.1, 80, 90, 100 Å$\}$ was applied.

The integrals between the atomic orbitals were calculated using the Gaussian 92 computer program [14] in STO-6G. STO-3G led to similar results. The input included the definition of the type of calculation for each point, the output format and the link to the next geometry. Then, the Gaussian 92 integrals between STO-6G orbitals were converted to integrals between Slater determinants with the formulae

$$\langle \| p\bar{q}r \| \boldsymbol{H}_{BO} \| s\bar{t}u \| \rangle = V_{NN}S_{ps}S_{qt}S_{ru}$$
$$- V_{NN}S_{pu}S_{qt}S_{rs} + I_{ps}S_{qt}S_{ru} + I_{qt}S_{ps}S_{ru}$$
$$+ I_{ru}S_{ps}S_{qt} - I_{pu}S_{qt}S_{rs} -$$
$$- I_{qt}S_{pu}S_{rs} - I_{rs}S_{pu}S_{qt} + (ps|qt)S_{ru}$$

$$+ (ps \mid ru)S_{qt} + (qt \mid ru)S_{ps} - (pu \mid qt)S_{rs} - (pu \mid rs)S_{qt} - (qt \mid rs)S_{pu}, \quad (2a)$$

$$\langle \| p\bar{q}r \| \, | \, \| s\bar{t}u \| \rangle = S_{ps}S_{qt}S_{ru} - S_{pu}S_{qt}S_{rs}, \quad (2b)$$

where $p, q, r, s, t, u \in \{a, b, c\}$. At this point the nuclear repulsion term V_{NN} is added with proper account of the variation of nuclear charges. Then the elements of $\mathbf{H}_{BO}$ and $\mathbf{S}$ are obtained by firstly converting the elements from the basis of Slater determinants to the basis of their unnormalized combinations $\varphi_i' = \varphi_i/N_i$ and finally by multiplication with the appropriate normalization factors which are obtained from the overlap integrals.

In the next steps, the Matlab computer program [15] was used to diagonalize the matrix $\mathbf{B}_{BO} - E\mathbf{S}$ at each point and to create the PESs. These were refined with a cubic interpolation procedure to a tenfold finer resolution. Test calculations at interpolated points ensured negligible energy deviations.

Known algorithms for finding the reaction coordinate on a calculated PES require an analytical expression for the ground state surface [16] or a recalculation of the energy during the search [17, 18]. For our case the following alternative routine was found convenient. The first point of the reaction coordinate is found for a large reactant distance of $r^0_{BC} = 6$ or 100 Å, respectively, with r^0_{AB} taken from the reactant geometry at the minimum ground state energy. During the reaction r_{BC} decreases whereas r_{AB} increases. By decreasing r_{BC} and increasing r_{AB}, simultaneously, one reaches three new positions $\{r^0_{BC} - 2d_{BC}, r^0_{AB}\}$, $\{r^0_{BC}, r^0_{AB} + 2d_{AB}\}$ and $\{r^0_{BC} - d_{BC}, r^0_{AB} + d_{AB}\}$ on the grid $\{d_{AB}, d_{BC}\}$. The lowest energy point of these is chosen as the second point on the RC, and this process is iterated until the product geometry is reached. This led to a completely reversible reaction path. The program then provided all VBCI energies along the reaction coordinate and the coefficients of the expansion of the states $\psi_i = \sum c_{ij}\varphi_j$.

The choice of the reference states for SCDs is somewhat arbitrary. It is clear that they must represent physically meaningful electron configurations [19] such as the eigenstates of the Born-Oppenheimer Hamiltonian at one given point of the RC [20]. Here, we adopt the VBCI states at the reactant geometry as logical reference states and refer to these states as diabatic and to the VBCI combinations as adiabatic. Instead of frozen reactant states other linear combinations can be chosen which lead to a more symmetrical SCD [4–6].

3 Results and discussion

3.1 The $H_2 + H$ reaction

It is illustrative to consider first the SCD arising from the interaction of the two covalent Heitler-London reference states $^1H_2 + H(\varphi_1)$ and $^3H_2 + H(\varphi_2)$ of the reactants because this already shows some essential features. The 2X2 VBCI problem has been solved analytically in previous work [3, 6, 12, 21], but with some approximations. For completeness we have now calculated the full solution retaining all overlap integrals. For the reactant (r), product (p), and the transition state (t) the wavefunctions are:

$$\psi_{1r} = \left(2\left(1 + S^2\right)\right)^{-1/2}\left\{\| a\bar{b}c \| + \| b\bar{a}c \|\right\}, \quad (3a)$$

$$\psi_{2r} = \left(6\left(1 - S^2\right)\right)^{-1/2}\left\{\| a\bar{b}c \| - \| b\bar{a}c \| + 2\| a\bar{c}b \|\right\}, \quad (3b)$$

$$\psi_{1p} = \left(2\left(1 + S^2\right)\right)^{-1/2}\left\{\| a\bar{b}c \| + \| a\bar{c}b \|\right\}, \quad (3c)$$

$$\psi_{2p} = \left(6\left(1 - S^2\right)\right)^{-1/2}\left\{\| a\bar{b}c \| - \| a\bar{c}b \| + 2\| b\bar{a}c \|\right\}, \quad (3d)$$

$$\psi_{1t} = \left(6\left(1 + S_1^2 - S_2^2 - S_1^2S_2\right)\right)^{-1/2} \left\{2\| a\bar{b}c \| + \| b\bar{a}c \| + \| a\bar{c}b \|\right\}, \quad (3e)$$

$$\psi_{2t} = \left(2\left(1 - S_1^2 + S_2^2 - S_1^2S_2\right)\right)^{-1/2} \left\{\| b\bar{a}c \| - \| a\bar{c}b \|\right\}, \quad (3f)$$

where $S = S_{ab}$ for the reactants, $S = S_{bc}$ for the products, and $S_1 = S_{ab} = S_{bc}, S_2 = S_{ac}$ for the transition state. They have the energies:

$$E_{1,2,r} = V_{NN} + I_{cc} + \left(1 \pm S^2\right)^{-1} \{I_{aa} + I_{bb} + (aa \mid bb) \pm (ab \mid ab) \pm 2I_{ab}S\}, \quad (4a)$$

$$E_{1,2,p} = E_{1,2,r} \text{ with (a) replaced by (c)}, \quad (4b)$$

$$E_{1,2,t} = \left(1 \pm S_1^2 \mp S_2^2 - S_1^2S_2\right)^{-1} \{K - M \pm (L_1 - L_2)\} \quad (4c)$$

where

$$K = 2I_{aa} + I_{bb} + 2(aa \mid bb) + (aa \mid cc)$$
$$M = (2I_{ab} + I_{ac})S_1^2 + 2(ab|ac)S_1 + (ab|bc)S_2 \quad (5)$$
$$L_1 = I_{aa}S_1^2 + (ab|ab) + 2(I_{ab} + (aa|bc))S_1$$
$$L_2 = I_{bb}S_2^2 + (ac|ac) + 2(I_{ac} + (bb|ac))S_2.$$

The energetically lower state ψ_i represents the bonding configurations $(^1H_2 + H)$ for the reactants and $(H + {}^1H_2)$ for the products, and their allylic superposition $(^1H_2 + H) + (H + {}^1H_2)$ for the transition geometry. The upper state ψ_2 is described by $(^3H_2 + H)$ and $(H + {}^3H_2)$ for reactants and products and yields a bond at the transition geometry between the outer atoms and an unpaired electron at the center [21]. Expression of ψ_p and ψ_t in terms of the reactant reference states ψ_r leads to

$$\psi_{1p} = \frac{1}{2\sqrt{2}}\left(\frac{2 - S^2}{1 + S^2}\right)^{1/2}\psi_{1r} + \frac{\sqrt{3}}{2\sqrt{2}}\left(\frac{2 + S^2}{1 + S^2}\right)^{1/2}\psi_{2r}, \quad (6a)$$

$$\psi_{2p} = \frac{\sqrt{3}}{2\sqrt{2}}\left(\frac{2 - S^2}{1 - S^2}\right)^{1/2}\psi_{1r} - \frac{1}{2\sqrt{2}}\left(\frac{2 + S^2}{1 - S^2}\right)^{1/2}\psi_{2r}, \quad (6b)$$

$$\psi_{1t} = \frac{\sqrt{3}}{2\sqrt{2}}\left(\frac{2 + S_1^2 - S_2^2 - 2S_1^2S_2}{1 + S_1^2 - S_2^2 - S_1^2S_2}\right)^{1/2}\psi_{1r} + \frac{1}{2\sqrt{2}}\left(\frac{2 - S_1^2 + S_2^2 - 2S_1^2S_2}{1 + S_1^2 - S_2^2 - S_1^2S_2}\right)^{1/2}\psi_{2r}, \quad (6c)$$

$$\psi_{2t} = \frac{1}{2\sqrt{2}}\left(\frac{2+S_1^2-S_2^2-2S_1^2S_2}{1-S_1^2+S_2^2-S_1^2S_2}\right)^{1/2}\psi_{1r} - \frac{\sqrt{3}}{2\sqrt{2}}\left(\frac{2-S_1^2+S_2^2-2S_1^2S_2}{1-S_1^2+S_2^2-S_1^2S_2}\right)^{1/2}\psi_{2r}\,, \qquad (6d)$$

with ψ_{1r} and ψ_{2r} normalized at the relevant geometries.

These equations show that the product ground state ψ_{1p} has a larger contribution of the excited reactant state ψ_{2r} than of the ground state ψ_{1r}, and the converse is true for ψ_{2p}. However, since both product states are linear combinations of both reactant states the transformations of ψ_{1p} into ψ_{2r} and of ψ_{2p} into ψ_{1r} as suggested by Fig. 1 are simplifications. This has been noticed before [6] and can be avoided by use of a different but less natural basis. For the linear transition geometry the ground state ψ_{1t} has a larger contribution of the reactant ground state than of the excited state, and the excited state ψ_{2t} is mostly composed of ψ_{2r}, as is intuitively expected.

Figure 2 shows the energies of the states ψ_1 and ψ_2 (full lines) and the energy expectation values of the reference states ψ_{1r} and ψ_{2r} (broken lines) along the reaction coordinate. As indicated by the representations in Eqs. (6a–d) the energies of the reference state do not reach the adiabatic energies at the product geometry. They do cross, though at a position which is slightly later than the transition state. Also, the energy splitting at the crossing point is not symmetric.

Inclusion of the zwitterionic and polar configurations φ_3–φ_8 [Eqs. (1c–h)] leads to a more complicated situation. For the reactant geometry the covalent configuration φ_1 mixes with the symmetric zwitterionic configuration φ_6. Therefore, appropriate linear combinations of these configurations were used as diabatic states besides the pure reactant configurations φ_2–φ_5, φ_7 and φ_8. Figure 3 shows the evolution of the calculated energies of these diabatic (upper part) and of the adiabatic (lower part) states along the RC. The behavior of the two lowest diabatic states is more symmetric than in Fig. 2 and closer to Fig. 1. Also, one clearly notices the Coulomb attraction for the charge transfer states $^sH_2^+ + H^-$ and $^sH_2^- + H^+$. They reach particularly low energies at the transition state geometry and are expected to mix strongly with the lower energy states. The positive energy excursions of the corresponding adiabatic states at the transition geometries confirm this expectation. In the full PES these charge transfer states show pronounced and extended energy minima at $r_{AB} = r_{BC} = 1.5$ Å and $r_{AB} = r_{BC} = 2.0$ Å, respectively, which we have not found described before.

The trends deduced from Eqs. (6a–d) and Figs. 2 and 3 are confirmed by the calculated expansion coefficients of the ground state $\psi_1 = \sum c_{1j}\varphi_j$ at selected points of the RC (Table 1).

From reactant to product the contribution of φ_1 decreases whereas that of φ_2 increases. At the transition geometry there are substantial contributions of the symmetric charge transfer configurations φ_3 and φ_5. For the reactant and product geometries the 8X8 VBCI coefficients are equivalent to

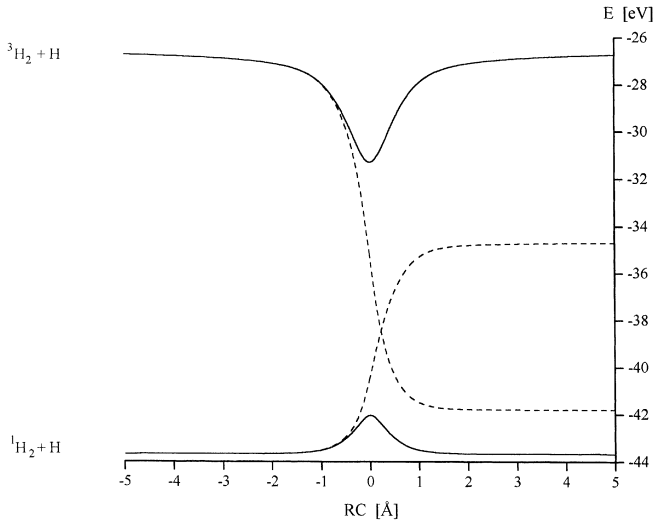

Fig. 2. Calculated SCD for the $H_2 + H$ reaction (2X2 VBCI, $\zeta = 1.24$)

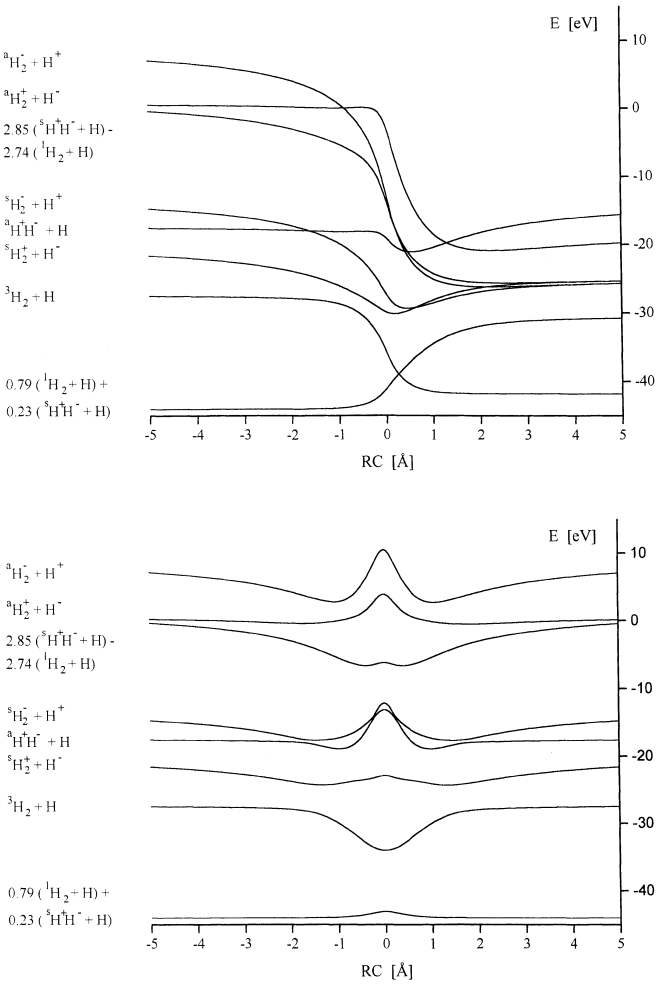

Fig. 3. Calculated SCD for the $H_2 + H$ reaction. *Upper part*: reference reactant states, *Lower part*: adiabatic states (8X8 VBCI, $\zeta = 1.24$)

Table 1. Expansion coefficients of the VBCI ground state Ψ_1 at selected geometries: r = reactants, p = products, t = transition state

Configuration	2X2 VBCI			8X8 VBCI		
	r	t	p	r	t	p
φ_1 $^1H_2$ + H	1	0.816	0.361	0.788	0.584	0.290
φ_2 $^3H_2$ + H	0	0.406	0.794	0	0.293	0.628
φ_3 $^sH_2^+$ + H^-				0	0.141	0.083
φ_4 $^aH^+H^-$ + H				0	−0.007	0
φ_5 $^sH_2^-$ + H^+				0	0.139	0.094
φ_6 $^sH^+H^-$ + H				0.226	0.155	0
φ_7 $^aH_2^+$ + H^-				0	0.010	0.083

$$\psi_{1r} = 0.4624\left(\| a\bar{b}c \| + \| b\bar{a}c \|\right) + 0.1330\left(\| a\bar{a}c \| + \| b\bar{b}c \|\right), \quad (7a)$$

$$\psi_{1p} = 0.4624\left(\| a\bar{b}c \| + \| a\bar{c}b \|\right) + 0.1330\left(\| a\bar{b}b \| + \| a\bar{c}c \|\right), \quad (7b)$$

i.e. necessarily the same superposition of covalent and zwitterionic configurations. Population analyses of the non-orthogonal basis states φ_i according to various methods [22] give the same result.

Table 2 displays the energies and bond lengths obtained in this and in previous work using different VBCI and MOCI methods. The first six rows show that optimization of the orbital exponents ζ decreases the absolute energy markedly whereas orbital floating has only a small effect. Inclusion of polar and zwitterionic configurations in the full VBCI lowers the barrier substantially. The results of a SCF MO QCISD calculation fully agree with the corresponding 8X8 VBCI data.

Our data also agree with the previous VBCI results of rows 7–9 but they are, as expected, quite far from the best theoretical and the experimental values. Of course, the VBCI calculations could be improved by enlarging the basis set. This would remove the deficiency of some unnaturally high energy states in Fig. 3 but cannot change the general interaction pattern of the lower states and the main conclusion, namely, that the polar charge transfer configurations contribute markedly to the transition state of even the $H_2 + H$ reaction. Although this was already contained in Hirschfelder's early results [23] it has not been clearly expressed before.

3.2 Modelling of substituent effects

In radical addition and abstraction reactions substituents of the radical and the substrate molecule alter the reaction enthalpy ($-H_r$) and the location of the excited reactant configurations [ΔE_{ST}, IP(R)-EA(M), IP(M)-EA(R)]. They are thought thereby to change the reaction barrier [3–8]. In quantum chemical models such effects may be simulated by core potentials at the substitution centers [12], and here this is modeled by setting the nuclear charges at A, B and C to $1 + q_A$, $1 + q_B$ and $1 + q_C$. For a total of 201 combinations $\{q_A = q,\ q_{B,C} = 0\}$, $\{q_B = q,\ q_{A,C} = 0\}$, $\{q_C = q,\ q_{A,B} = 0\}$, $\{q_A = q = \pm q_B,\ q_C = 0\}$, $\{q_A = q = \pm q_C,\ q_B = 0\}$, $\{q_B = q = \pm q_C,\ q_A = 0\}$, $\{q_{A,C} = q_1,\ q_B = q_2\}$, $\{q_{A,B} = q_1,\ q_C = q_2\}$, $\{q_{A,B,C} = 0\}$ and q, q_1, $q_2 = \pm 0.1, \pm 0.05$, ± 0.02 and ± 0.01, the PESs and SCDs were calculated using the 8X8 VBCI routine as before with the STO-6G basis, standard ζ and no orbital floating. The large number of calculations does not allow discussion of the results individually. Hence, most of them are presented and discussed globally, in particular with respect to the desired correlations of the barrier properties with H_r and the reactant state energies. Also, some data for thermo-

Table 2. Energies and bond lengths for the H_2+H reaction

Method	E_H [eV]	E_{H_2} [eV]	r_{H_2} [Å]	BE_{H_2} [KJ/Mol]	E_{TS} [eV]	r_{TS} [Å]	BE_{TS} [KJ/Mol]	E_0 [KJ/Mol]
2X2 VBCI, $\zeta = 1.24$	−12.82	−30.86	0.704	502.8	−42.03	0.909	344.6	158.2
2X2 VBCI, ζ_{opt} [a]	−13.60	−30.99	0.749	363.3	−43.25	1.033	235.1	128.2
8X8 VBCI, ζ = 1.24	−12.82	−31.18	0.733	533.5	−43.07	0.934	444.1	89.4
8X8 VBCI, ζ_{opt} [b]	−13.60	−31.23	0.756	386.5	−43.81	0.997	288.9	97.6
8X8 VBCI, ζ_{opt}, float[c]	−13.60	−31.29	0.756	392.7	−43.84	0.999	291.4	101.4
MO QCISD[d]	−13.60	−31.23	0.757	387.1	−43.84	1.009	291.5	95.6
Hirschfelder, 1936[e]			0.751	385.9		0.974	280.7	105.2
Linnett, 1966[f]					−43.9	1.00		92.1
Klessinger, 1983[g]						0.979		98
Liu, 1984[h]	−13.60	−31.96	0.741	457.4	−45.14	0.930	417.1	40.1
Exp[i]	−13.60	−31.96	0.741	458	−45.14		421	40

[a] Reactants: $\zeta_{a,b} = 1.166$, $\zeta_c = 0.999$; transition state: $\zeta_{a,c} = 1.053$, $\zeta_b = 1.079$
[b] Reactants: $\zeta_{a,b} = 1.194$, $\zeta_c = 1.000$; transition state: $\zeta_{a,c} = 1.060$, $\zeta_b = 1.203$
[c] Floating orbitals and optimized ζ; reactants: $\zeta_{a,b} = 1.190$, $\zeta_c = 0.999$, $r_{ab} = 0.716$ Å; transition state: $\zeta_{a,c} = 1.055$, $\zeta_b = 1.215$, $r_{ab} = r_{ba} = 0.984$ Å
[d] MO QCISD/STO-6G with optimized ζ from[b]
[e] 4X4 VBCI: reactants: $\zeta_{a,b,c} = 1.193$; transition state: $\zeta_{a,b,c} = 1.087$, integrals calculated explicitely; see Ref. [23]
[f] 8X8 VBCI: transition state: $\zeta_{a,c} = 1.06$, $\zeta_b = 1.21$, some integrals approximated; see Ref. [27]
[g] 2X2 VBCI with optimized ζ and floating orbitals, integrals approximated; see Ref. [12]
[h] From Ref. [11]
[i] From Ref. [28]

neutral reactions are not shown since they did not provide significant additional information.

Figure 4 confirms one of the major predictions derived from the SCD. Apart from a few numbered cases which will be discussed later on the reaction barrier decreases with increasing exothermicity ($-H_r$). A linear regression gave $E_a = 0.90 + 0.53H_r (R^2 = 0.76)$. Interestingly, its slope is very similar to the slopes of 0.40–0.56 calculated for the addition of several alkyl radicals to alkenes with high-level MO methods by Wong et al. [7]. Experimentally somewhat lower slopes of 0.21–0.26 have been found [8]. Also as expected from the qualitative SCD, the distance of the approaching centers r_{BC} in the transition state decreases with increasing reaction endothermicity H_r (Fig. 5), i.e the transition state becomes later for the more endothermal reactions. The linear correlation is expressed by $r_{BC} = 0.935 - 0.065\ H_r\ (R^2 = 0.76)$ where r_{BC} is given in Å and H_r in eV. Again, by high-level MO calculations on polyatomic systems similar dependences have been found [7], though with different slopes. These may reflect the much looser transition state for the addition reactions considered by Wong et al.

The SCD also predicts that E_0 and r_{BC} at the transition state should depend on the singlet-triplet splitting ΔE_{ST}. A decrease of r_{BC} with increasing ΔE_{ST} was indeed found but no clear correlation of E_0 with this parameter was obtained, which may be due to the limitations of the model.

On the other hand, the effects of low-lying charge transfer states are clearly recognized. Figure 6 shows E_0 as a function of the energy gaps between the ground state and the reactant states $AB^+ + C^-$ and $AB^- + C^+$. The numbered points are the same as in Fig. 4, and it is now obvious that the particularly low barriers for these numbered cases originate from particularly large charge transfer contributions which stabilize the transition state. This is confirmed by correspondingly large coefficients (0.20 – 0.26) of the charge transfer configurations in the transition state wavefunction.

For the large combination $q_A = q_B = -0.1$, $q_C = +0.1$, which corresponds to point 1 in Figs. 4 and 6, the state correlation diagram is shown in Fig. 7. Due to the stabilization of AB^+ the reactant charge transfer configuration $^sAB^+ + C^-$ now has a lower energy than the unpolar triplet state $^3AB + C$. In the transition region there are two avoided crossings of low energy states. Interestingly, this has little effect on the behavior of the lowest adiabatic states, i.e. the schematic SCD of Fig. 1 is obeyed even in such extreme cases.

From the examples above it is clear that enthalpic and polar charge transfer effects both influence the reaction barrier, so that a separation would be desirable. For addition reactions of nucleophilic radicals with electron-deficient alkenes this was found difficult [7, 8] because the electron affinities of the alkenes correlate with the reaction exothermicity, and the enthalpy and polar effects parallel each other. Here, the same correlation is found for the systems with low IP(C)-EA(AB) which are represented by the points 1′–4′ in Figs. 4 and 6 i.e. a clear separation of polar and enthalpic effects was not achieved. However, for the case of low IP(AB)-

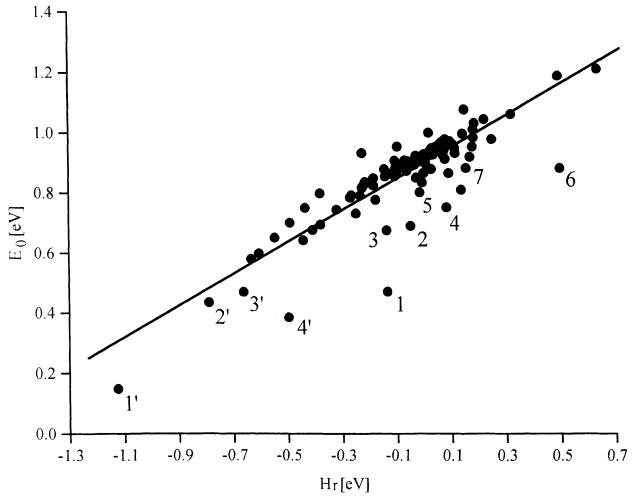

Fig. 4. Reaction barrier versus reaction enthalpy. Numbered points refer to systems with large charge transfer

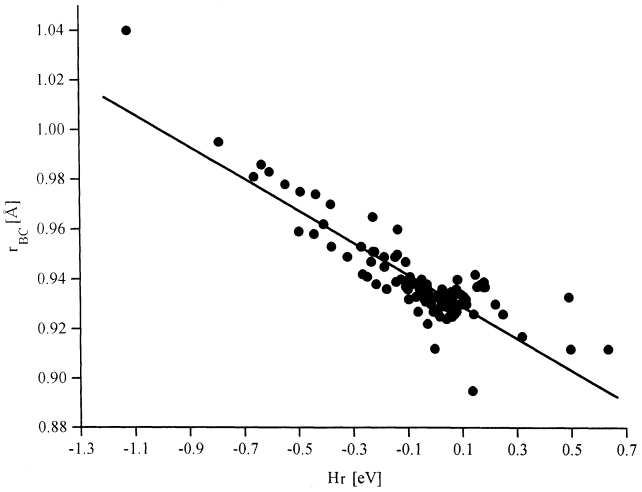

Fig. 5. Reaction distance versus reaction enthalpy

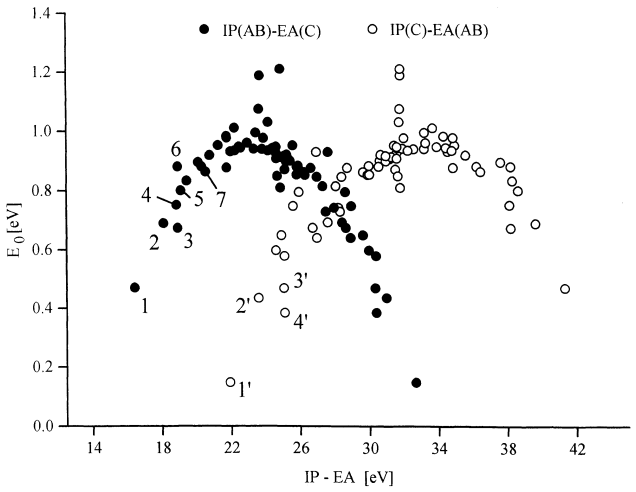

Fig. 6. Reaction barrier versus polar states energies

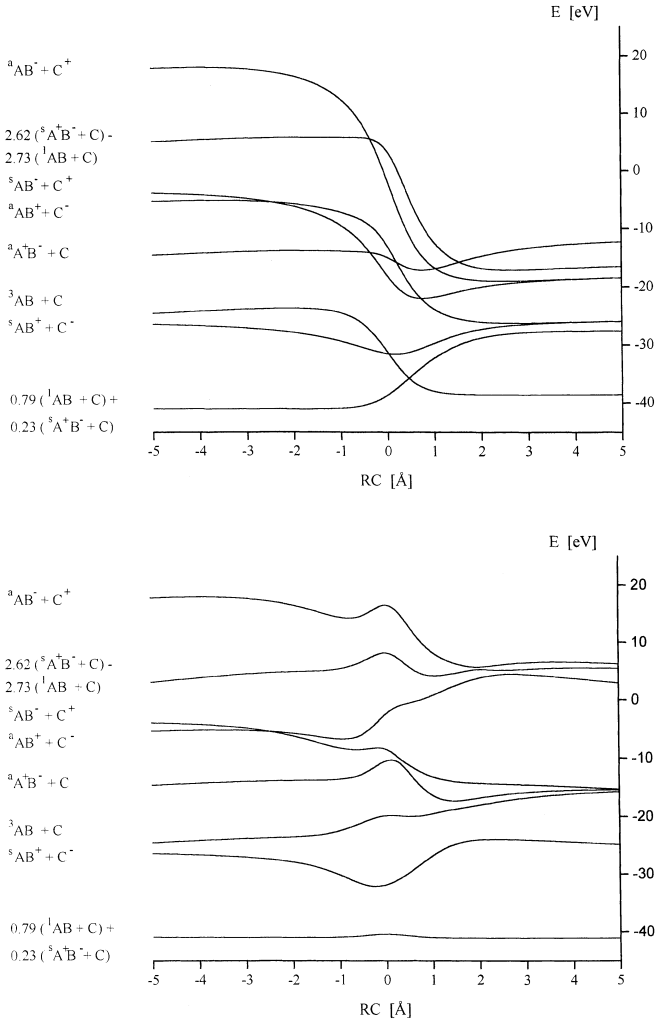

Fig. 7. Calculated SCD for the $AB + C \rightarrow A + BC$ with $Z_A = Z_B = 1.1$, $Z_C = 0.9$. *Upper part*: reference reactant states. *Lower part*: adiabatic states (8X8 VBCI, $\zeta = 1.24$)

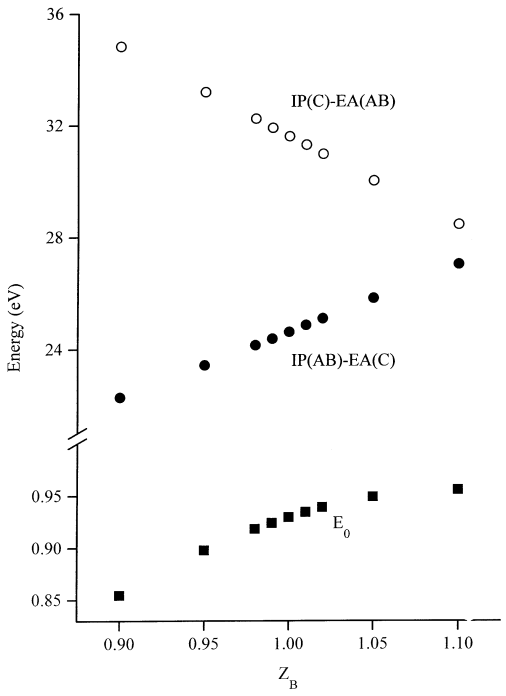

Fig. 8. Calculated energies of the reactant charge transfer states and the reaction barrier E_0 for the nuclear charges $Z_A = Z_C = 1$, i.e. A = C = H, and various values of Z_B

EA(C), i.e. strongly electrophilic radicals reacting with electron-rich substrates no correlation of IP(AB) with H_r was obtained. This is compatible with the surprisingly good correlations of rate constants for the addition of several fluoroalkyl radicals to electron-rich alkenes with the alkenes IP [9].

Finally, we note that the VBCI calculations also correctly model the general reactivity pattern of the hydrogen atom. From Hammett $\rho\sigma$ relations this is known to be slightly electrophilic in abstraction reactions from substituted toluenes and in addition reactions to substituted aromatic and heterocyclic compounds [24]. Rate constants for the hydrogen addition to haloalkenes in the gas phase [25] and the partial electron transfer from the substrate to the hydrogen atom found in calculated transition states for the addition to ethene, vinylamine and ethine [26] support this view. In our modeling of substituent effects by variation of nuclear charges, the electrophilicity is most clearly expressed by results obtained for the set of charges $Z_A = Z_C = Z_H = 1$ and Z_B variable. For these cases the reaction is thermoneutral, and any variation of E_0 with the nuclear charge of the transferred atom B must be mainly due to polar effects. Figure 8 shows that the energy of the lower charge transfer state $AB^+ + C^-$ decreases with decreasing Z_B whereas that of the higher state $AB^- + C^+$ increases as a natural consequence of the decreasing Coulomb attraction for atom B. The barrier E_0 also decreases due to the larger contribution of $AB^+ + C^-$. This is in accord with the electrophilic behavior but in comparison to the data given in Figs. 4 and 6 the variations of E_0 are small, i.e. the hydrogen atom is also calculated to be only slightly electrophilic as observed.

4 Conclusion

In summary, the VBCI results on the three-electron three-center model strengthen the utility of the intuitively created SCD of Fig. 1 in discussions of factors which influence radical abstraction and addition reactions and reveal some simplifications involved in its construction. They also show that charge transfer configurations are generally important for the exact theoretical description of transition states, and this agrees with the established need for extensive configuration interaction in high-level ab initio molecular orbital calculations [7]. The large influence of the reaction enthalpy on the reaction barriers is confirmed, and it is also demonstrated that in favorable cases polar substituent effects can become dominant. Further, the weak electrophilicity of the hydrogen atom in addition and abstraction reactions is correctly simulated.

Acknowledgements. We acknowledge the advice of Prof. K. M. Salikhov (Kazan), helpful discussions with Prof. L. Radom (Canberra) and Prof. W. Thiel (Zurich) and financial support from the Swiss National Foundation for Scientific Research.

References

1. Longuet-Higgins HC, Abrahamson EW (1965) J Am Chem Soc 87:2045
2. Yamaguchi K (1974) Chem Phys Lett 28:93
3. Bonačič-Koutecký V, Koutecký J, Salem L (1977) J Am Chem Soc 99:842
4. Shaik SS, Canadell E (1990) J Am Chem Soc 112:1446; Shaik SS (1991) Pure Appl Chem 63:195
5. Pross A, Yamataka H, Nagase S (1991) J Phys Org Chem 4:135
6. Shaik SS, Hiberty PC, Lefour J-M, Ohanessian G (1987) J Am Chem Soc 109:363; Shaik SS, Hiberty PC, Ohanessian G, Lefour J-M (1988) J Phys Chem 92:5086; Maitre P, Hiberty PC, Ohanessian G, Shaik SS (1990) J Phys Chem 94:4089
7. Wong MW, Pross A, Radom L (1993) J Am Chem Soc 115:11050, (1994) Isr J Chem 33:415, (1994) J Am Chem Soc 116:6284, (1994) J Am Chem Soc 116:11938
8. Münger K, Fischer H (1985) Int J Chem Kinet 17:809; Héberger K, Fischer H (1993) Int J Chem Kinet 25:249, (1993) Int J Chem Kinet 25:913; Wu JQ, Fischer H (1995) Int J Chem Kinet 27:167; Wu JQ, Beranek I, Fischer H (1995) Helv Chim Acta 78:194; Walbiner M, Wu JQ, Fischer H (1995) Helv Chim Acta 78:910; Salikhov A, Fischer H (1993) Appl Magn Reson 5:445; Zytowski T, Fischer H (1996) J Am Chem Soc 118:437; Batchelor SN, Fischer H (1996) J Phys Chem 100:9794
9. Avila DV, Ingold KU, Lusztyk J, Dolbier WR Jr Pan H-Q (1993) J Am Chem Soc 115:1577; Avila DV, Ingold KU, Lusztyk J, Dolbier WR Jr Pan H-Q, Muir M (1994) J Am Chem Soc 116:99; Avila DV, Ingold KU, Lusztyk J, Dolbier WR Jr Pan H-Q (1996) J Org Chem 61:2027
10. London F (1929) Z Elektrochem 35:552
11. Liu B (1984) J Chem Phys 80:581; Siegbahn P, Liu B (1978) J Chem Phys 68:2457; Varandas AJC, Brown FB, Alden Mead C, Truhlar DG, Blais NC (1987) J Chem Phys 86:6258; Boothroyd Al, Keogh WJ, Martin PG, Peterson MR (1991) J Chem Phys 95:4343
12. Höweler U, Klessinger M (1983) Theor Chim Acta 63:401, (1985) Theor Chim Acta 67:485; Klessinger M, Höweler U (1986) J Mol Struct 138:151
13. Gerhartz W, Poshusta RD, Michl J (1976) J Am Chem Soc 98:6427, (1977) 99:4263, (1977) 99:4263
14. Frisch MJ, Trucks GW, Schlegel HB, Gill PMW, Johnson BG, Wong MW, Foresman JB, Robb MA, Head-Gordon M, Replogle ES, Gomperts R, Andres JL, Raghavachari K, Binkley JS, Gonzalez C, Martin RL, Fox DJ, Defrees DJ, Baker J, Stewart JJP, Pople JA (1993) Gaussian 92/DFT, Revision F2. Gaussian Inc., Pittsburgh, Pa
15. Matlab, reference guide (1992) The Math Works Inc., Cochitue Place
16. Halgren TA, Lipscomb WN (1977) Chem Phys Lett 49:225
17. Warshel A, Weiss RM (1980) J Am Chem Soc 102:6218
18. Schlegel HB (1992) Theor Chim Acta 83:15, (1994) J Chem Soc Faraday Trans 90:1569
19. O'Malley TF (1971) Adv At Mol Phys 7:223; Carrington T (1974) Acc Chem Res 7:20
20. Whetten RL, Ezra GS, Grant ER (1985) Annu Rev Phys Chem 36:277
21. Slater JC (1931) Phys Rev 38:1109; Hirschfelder JO (1938) J Chem Phys 6:795; Porter RN, Karplus M (1964) J Chem Phys 40:1105; Eyring H, Lin SH, Lin SM (1980) Basic chemical kinetics. Wiley, New York pp 27–30 and references therein
22. Chirgwin BH, Coulson CA (1950) Proc R Soc 201A:196; Peters D (1962) J Am Chem Soc 84:3812; Löwdin P-O (1974) Ark Mat Astr Fysik 35A:9; Gallup GA, Norbeck JM (1973) Chem Phys Lett 21:495; Norbeck JM, Certain PR (1975) J Chem Phys 63:4127
23. Hirschfelder J, Eyring H, Rosen N (1936) J Chem Phys 4:121
24. Pryor WA, Lin TH, Stanley JP, Henderson RW (1973) J Am Chem Soc 95:6993 and references therein
25. Ahmed MG, Jones WE (1985) Can J Chem 63:2127
26. Nagase S, Kern CW (1979) J Am Chem Soc 101:2544, (1980) J Am Chem Soc 102:4513; Delbecq F, Ilavsky D, Anh NT, Lefour JM (1985) J Am Chem Soc 107:1623
27. Bowen HC, Linnett JW (1966) Trans Faraday Soc 62:2953
28. Chase MW Jr, Davis CA, Downey JR Jr, Frurip DJ, McDonald RA, Syverud AN (1985) J Phys Chem Ref Data 14 [Suppl 1]; Herzberg G (1964) Spectra of diatomic molecules. Van Nostrand, New York; Stoicheff BP (1957) Can Phys 35:730; Schulz WR, Le Roy DJ (1965) J Chem Phys 42:3869